Scientific Research Publishing

Atmospheric and Climate Sciences, 2022, 12, 588-602
https://www.scirp.org/journal/acs
ISSN Online: 2160-0422
ISSN Print: 2160-0414

Vertical Profile Comparison of Aerosol and Cloud Optical Properties in Dominated Dust and Smoke Regions over Africa Based on Space-Based Lidar

Didier Ntwali[1], Getachew Dubache[2], Faustin Katchele Ogou[3]

[1]Rwanda Space Agency (RSA), Earth and Space Science Division, Kigali, Rwanda
[2]College of Reading Academy, Nanjing University of Information Science and Technology, Nanjing, China
[3]Laboratory of Atmospheric Physics, Department of Physics, University of Abomey-Calavi, Abomey-Calavi, Benin
Email: dntwali@space.gov.rw, gechdubache@yahoo.com, ogofaustin@gmail.com

How to cite this paper: Ntwali, D., Dubache, G. and Ogou, F.K. (2022) Vertical Profile Comparison of Aerosol and Cloud Optical Properties in Dominated Dust and Smoke Regions over Africa Based on Space-Based Lidar. *Atmospheric and Climate Sciences*, **12**, 588-602.
https://doi.org/10.4236/acs.2022.123033

Received: April 19, 2022
Accepted: July 9, 2022
Published: July 12, 2022

Abstract

This study evaluates the vertical profiles of aerosol and cloud optical properties in 40 dominated dust and smoke regions in Western-Northern Africa (WNA) and Central-Southern Africa (CSA), respectively, from the surface to 10km and from 2008 to 2011 based on LIVAS (LIdar climatology of Vertical Aerosol Structure for space-based lidar simulation studies). Aerosol extinction (AE), aerosol backscatter (AB), and aerosol depolarization (AD) generally increase from the surface to 1.2 km and decrease from 1.2 km to the upper layers in both WNA and CSA. AE and AB in CSA (maximum of 0.13 km^{-1}, 0.14 km^{-1}, 0.0021 $km^{-1}\cdot sr^{-1}$, 0.0033 $km^{-1}\cdot sr^{-1}$) are higher than in WNA (maximum of 0.07 km^{-1}, 0.08 km^{-1}, 0.0017 $km^{-1}\cdot sr^{-1}$, 0.0015 $km^{-1}\cdot sr^{-1}$) at 532 and 1064 nm respectively. AD in WNA (maximum of 0.25) is significantly higher than in CSA (maximum of 0.05). There is a smooth change with the height of cloud extinction and backscatter in WNA and CSA, while there is a remarkable increase of cloud depolarization with height, whereby it is high in CSA and low in WNA due to high and low fraction of cirrus respectively. Altocumulus has the highest extinction in NA (0.0139 km^{-1}), CA (0.058 km^{-1}), WA (0.013 km^{-1}), while low overcast transparent (0.76 km^{-1}) below 1 km in SA. The major findings of this study may contribute to the improvement of our understanding of aerosol-cloud interaction studies in dominated dust and smoke aerosol regions.

Keywords

Vertical Profile, Dust Aerosols, Smoke Aerosols, Clouds, Africa, Lidar

Climatology of Vertical Aerosol Structure for Space-Based Lidar Simulation Studies (LIVAS)

1. Introduction

Active sensors and atmospheric models have been used to analyse vertical structure, aerosol, and cloud optical properties at global scale, however, few studies have investigated the African climatology aspect at high spatial scale. As a result, the knowledge on the quantification of the impacts of aerosols on the radiation budget and cloud processes remains poor. The atmospheric aerosols are broadly classified as natural (wind-borne desert dust, sea spray, volcanic eruptions, forest fire, etc.) and anthropogenic (biomass burning activities, industrial and urban pollution, fossil fuels combustion, car traffic, etc.) aerosols. The dust and biomass-burning aerosol are remarkably concentrated in Western-Northern Africa (WNA) and Central-Southern Africa (CSA) respectively in all seasons [1]. The largest fractions of dust in the world are found in Sahara desert [2]-[7] while the largest amount of biomass burning is found in South Africa [8] [9], and Africa is the continent with the largest number of fires from biomass burning [9] [10]. A recent study also showed that Central and South Africa are among the regions in the world with the largest fraction of biomass-burning aerosols [11]. This shows the tangible fact that dust and biomass burning aerosol studies are essential in the Saharan and Sahel regions in West and North of Africa and Central and South of Africa regions, respectively.

The sophisticated lidars are highly needed in many regions of Africa to have more knowledge on aerosol and cloud studies. The aerosol types are classified by their hygroscopicity and chemically by their predominant species [12]. Such classification is very useful for aerosol and cloud interaction studies.

The LIVAS (LIdar climatology of Vertical Aerosol Structure for space-based lidar simulation studies) provides six aerosol type data from the simulation of CALIOP (Cloud-Aerosol Lidar with Orthogonal Polarization) on board of CALIPSO (Cloud-Aerosol Lidar and Infrared Pathfinder Satellite Observations) layer 2 data products [13]. The six aerosol types defined by CALIPSO are clean continental, clean marine, dust, polluted continental, polluted dust, and smoke, which are determined by the attenuated backscatter, volume depolarization ratio, surface type and layer height [12]. The Lidar is a particularly useful instrument which gives us insight into the detailed vertical distribution of the aerosol optical properties [14] [15] [16] [17] [18]. There is an agreement between LIVAS and CALIPSO in polluted continental types, while for smoke particles the LIVAS shows a large number of fine particles whereas CALIPSO indicates the same volume distribution of both fine and coarse particles [14]. They also reported that the LIVAS has fewer fine particles than CALIPSO for dust particles, while there is an agreement between LIVAS and AERONET on the average size distribution

of both smoke and dust particles.

The aerosol optical properties were found to be accurate at 355 nm and 532 nm [4]. The dust aerosols are lifted up due to strong winds and then transported over long distances [7] [19] [20]. The smoke particles have high absorption and result in radiative heating ([21] Keil and Haywood, 2003; [22]. There are significant smoke aerosols in Central and South Africa and their sources [23]. Saharan dust particles show Africa also some absorption of solar radiation leading to local warming of the atmosphere [22]. The dust and smoke backscatter coefficients were found almost equal at 532 nm, while the smoke extinction coefficient was found higher than that of dust [24]. The backscatter coefficient was found to be sensitive to the shape of dust particles [4]. The aerosol extinction coefficient is weakly influenced by the shape of aerosols, while the aerosol backscatter coefficient is strongly reduced by non-spherical dust particles [15] [25].

The aerosol composition changes their size distributions and refractive indices due to the variability of relative humidity [26]. The continental aerosol components were found to grow with the increase of relative humidity [26]. The highly stratified aerosol layers of dust and smoke up to 5.5 km in height were found close to Africa [27]. There exists a high concentration of biomass burning particles in dust during winter due to savanna fires in the Sahel [28].

The backscatter coefficients were found to be high and low for dust in the shape of sphere and spheroid, respectively [4]. The mixing of dust and smoke aerosols was found in many previous studies. In this paper, we focus only on two dominant aerosol types in Western-Northern Africa (WNA) and Central-Southern Africa (CSA) regions, namely, dust and smoke.

Our contribution is to identify the variability of vertical profiles of smoke and dust aerosols in terms of their optical properties in WNA and CSA. There are two main goals of this study: the first is to investigate and compare the vertical profiles of aerosol and cloud optical properties in dominated dust and smoke regions in Africa. The 40 regions were selected due to their location known to have large dust and biomass-burning aerosols. This is the first study related to the vertical profiles of aerosol and cloud properties in many Africa regions with few or lack of ground-based instruments. The second goal is to investigate the relationship between the vertical structure of aerosol and cloud optical properties in dominated dust and smoke regions.

The 40 regions evaluated are located from 12˚N to 28˚N and 18˚W to 21˚E in WNA, while from 1˚S to 34˚S and 12˚E to 35˚E in CSA. The paper is organized as follows. The data and methodology used in this study are described in Section 2, and the results obtained are discussed in Section 3. In Section 4, we present new findings and concluding remarks.

2. Data and Methodology

2.1. Data

The LIVAS (LIdar climatology of Vertical Aerosol Structure for space-based li-

dar simulation studies) provides data for vertical structure of aerosol and cloud optical properties on a global scale from CALIPSO (Cloud Aerosol Lidar and Infrared Pathfinder Satellite Observations) observations at 532 nm and 1064 nm and depends on the aerosol types for spectral conversion factors of extinction and backscatter derived from European Aerosol Research Lidar Network (EARLINET) [13]. The LIVAS is a 3-dimensional global vertical aerosol structure dataset sponsored by the European Space Agency (ESA) [29]. LIVAS uses level 2 (version 3) product of CALIOP (Cloud-Aerosol Lidar with Orthogonal Polarization) sensor on board CALIPSO satellite [13], in which CALIPSO (level 2) has the ability to determine the vertical profiles of aerosols and clouds [30] and to distinguish aerosols from clouds [31]. The LIVAS data have been used in this study over a period of 4 years from 2008 to 2011 as the climatology aspect. LIVAS provides monthly data with a spatial resolution of 1 × 1 degree, vertical resolution from 60 m (between −0.5 km and 21 km) to 180 m (above 21 km) [13]. The LIVAS data are very useful for satellite sensors and model performance evaluation [29] and have shown good agreement with AERONET at a global scale in the previous study by Amiridis *et al.* [13]. The users are recommended to consider grids for which the number of CALIPSO overpasses is greater than 150 [13]. In this study, we have also considered grids with the number of CALIPSO overpasses less than 150 to capture the aerosol events as much as possible.

2.2. Methodology

We have analysed the vertical structure of aerosol and cloud optical properties in 20 regions located in Western-Northern of Africa (WNA) and the other 20 regions in Central-Southern of Africa (CSA) as shown in **Table 1**. The 40 regions were selected and chosen by default but focusing on regions dominated by dust and biomass burning regions in Western-Northern of Africa and Central-Southern Africa respectively (**Figure 1**).

The method used by Amiridis *et al.* [13] is that for the conversions applied in LIVAS, the spectral dependence of the extinction and backscatter is considered to follow the well-known Ångström exponential law as follows:

$$x_{par}\left(\lambda_2\right) = x_{par}\left(\lambda_1\right)\left(\frac{\lambda_1}{\lambda_2}\right)^{\dot{A}_{\lambda_1/\lambda_2}}$$

where $x_{par}(\lambda_2)$ is the converted extinction or backscatter at λ_2 (either 355, 1570 or 2050 nm), $\dot{A}_{\lambda_1/\lambda_2}$ is the extinction or backscatter-related Ångström exponent and $x_{par}(\lambda_1)$ is the extinction or backscatter product of CALIPSO at λ_1 = 532 nm.

The LIVAS allowed us to analyze six properties, namely, aerosol extinction coefficient and aerosol backscatter coefficient at both 532 nm and 1064 nm, and aerosol depolarization ratio, cloud extinction coefficient, cloud backscatter coefficient, and cloud depolarization ratio at 532 nm. The aerosol and cloud subtypes data are retrieved at 532 nm. The largest fractions of dust in the world are found in Sahara desert [5] [6] [7], while the largest amount of biomass burning is found in Southern Africa [8] [9] and Africa is the continent with the largest

number of fires from biomass burning [9] [10]. A large fraction of mineral dust aerosols is found over Sahara desert [4] in Western Africa [32] [33]. A recent study also showed that Central and Southern Africa are among the regions in the world with the largest fraction of biomass burning aerosols [11]. This shows that the Saharan desert and Sahel regions in Western and Northern Africa and Central and Southern Africa regions are the best regions for dust and biomass burning smoke aerosol studies, respectively. Due to the different aerosol and cloud type spatial distribution in Western, Northern, Central, and Southern Africa [34], we have evaluated the aerosol and cloud optical properties relationships in those regions. The LIVAS provides regional and seasonal statistics of aerosol and cloud optical properties [13]. We have used LIVAS statistical mean data of aerosol-cloud optical properties and aerosol-cloud subtypes for 4 years. The LIVAS provides the statistical mean related to the surface elevation, the number

Table 1. Description of 40 regions in WNA and CSA selected for the vertical profiles of aerosol and cloud optical properties.

20 Regions in Western-Northern of Africa (WNA)				20 Regions in Central-Southern of Africa (WNA)			
	Number of CALIPSO Overpasses	Lat	Lon		Number of CALIPSO Overpasses	Lat	Lon
Adrar	165	26.5	−1.5	Durban	165	−29.5	30.5
Agadez	78	19.5	10.5	Gorogonsa	86	−18.5	34.5
Agoufou	98	15.5	−1.5	Johannesburg	164	−26.5	28.5
Al Kufrah	170	23.5	22.5	Kadoma	81	−18.5	29.5
Banizoumbou	82	13.5	2.5	Kasai	159	−4.5	21.5
Dakar	167	14.5	−17.5	Kinshasa	82	−4.5	15.5
Ennedi	108	18.5	21.5	Kolwezi	83	−10.5	25.5
Ghat	85	25.5	10.5	Luanda	37	−9.5	13.5
Hodh El Chargui	166	18.5	−7.5	Lubumbashi	174	−11.5	27.5
Hodh El Gharbi	162	16.5	−9.5	Lusaka	166	−15.5	28.5
Illizi	100	26.5	7.5	Maputo	98	−25.5	32.5
Kidal	159	19.5	0.5	Mongu	165	−15.5	23.5
Matam	79	15.5	−13.5	Muchungue	158	−20.5	33.5
Murzuq	139	24.5	15.5	North-Western of Rwanda	166	−1.5	29.5
Ouagadougou	161	12.5	−1.5	North-Western of Burundi	167	−3.5	29.5
Tamnrasset	160	23.5	4.5	Pietermaritzburg	166	−29.5	29.5
Tibesti	166	21.5	16.5	Port Elizabeth	82	−33.5	25.5
Tindouf	168	27.5	−6.5	Pretoria	164	−25.5	28.5
Tirris Zemmour	88	24.5	−9.5	SEGC Lope	165	−0.5	12.5
Tombouctou	171	20.5	−4.5	Skukuza	83	−24.5	30.5

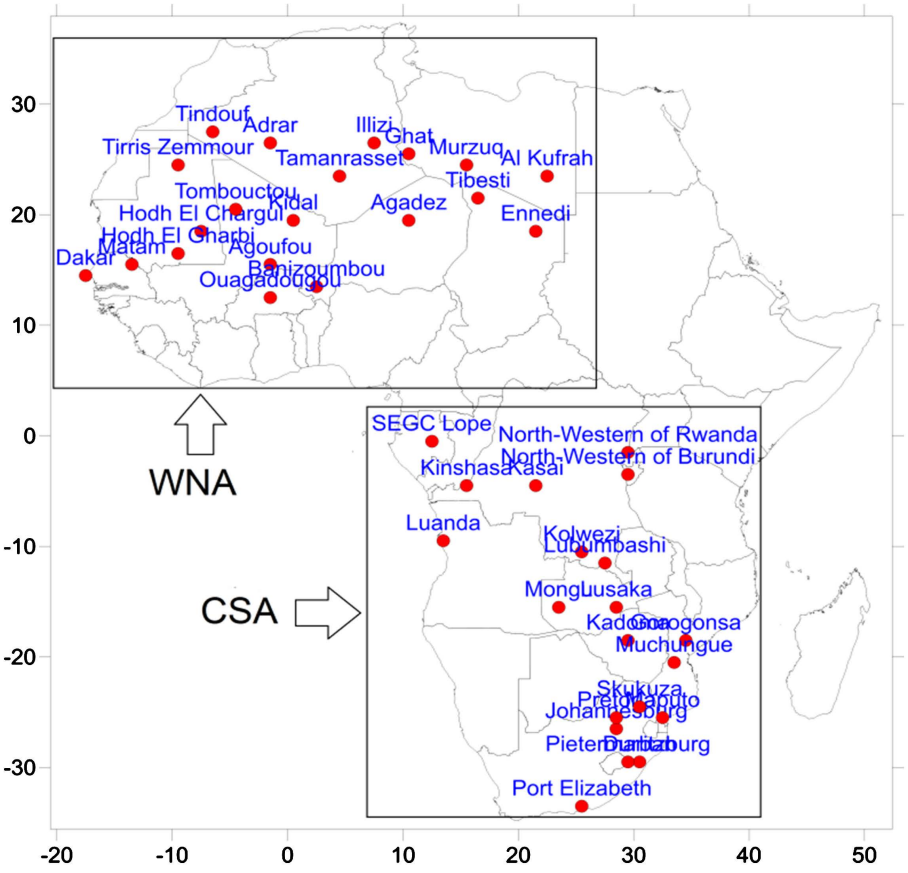

Figure 1. Location of 40 regions selected in West-North of Africa (WNA) and Central-South of Africa (CSA) for the vertical profiles of aerosol and cloud optical properties.

of CALIPSO overpasses, number of profiles examined, and samples averaged after filtering (aerosol, clear air, total) for each grid cell [13].

3. Results

The dust and biomass burning aerosol particles have different light absorbing and scattering properties [27]. The aerosol properties such as shape, size distribution, and composition influence their scattering characteristics [35]. The source of dust aerosols may strongly affect their optical properties [36]. The aerosol subtypes with high extinction values are dust aerosols in both Northern Africa (maximum of 0.045 km^{-1}) (**Figure 2(a)**) and Western Africa (maximum of 0.088 km^{-1}) (**Figure 2(b)**) while significant high extinction of smoke aerosols in both Central Africa (maximum of 0.0014 km^{-1}) (**Figure 2(c)**) and Southern Africa (maximum of 0.0011 km^{-1}) (**Figure 2(d)**). The dust and smoke aerosols vertical distributions reveal the impacts of aerosols on several cloud types. The dust and smoke aerosols may have different impacts on clouds due to their different optical, physical, and chemical properties. The clean marine, polluted continental, and clean continental aerosol subtypes have a remarkable low extinction in NA (**Figure 2(a)**), WA (**Figure 2(b)**), and CA (**Figure 2(c)**), while there are much less dust and clean continental aerosols in SA (**Figure 2(d)**).

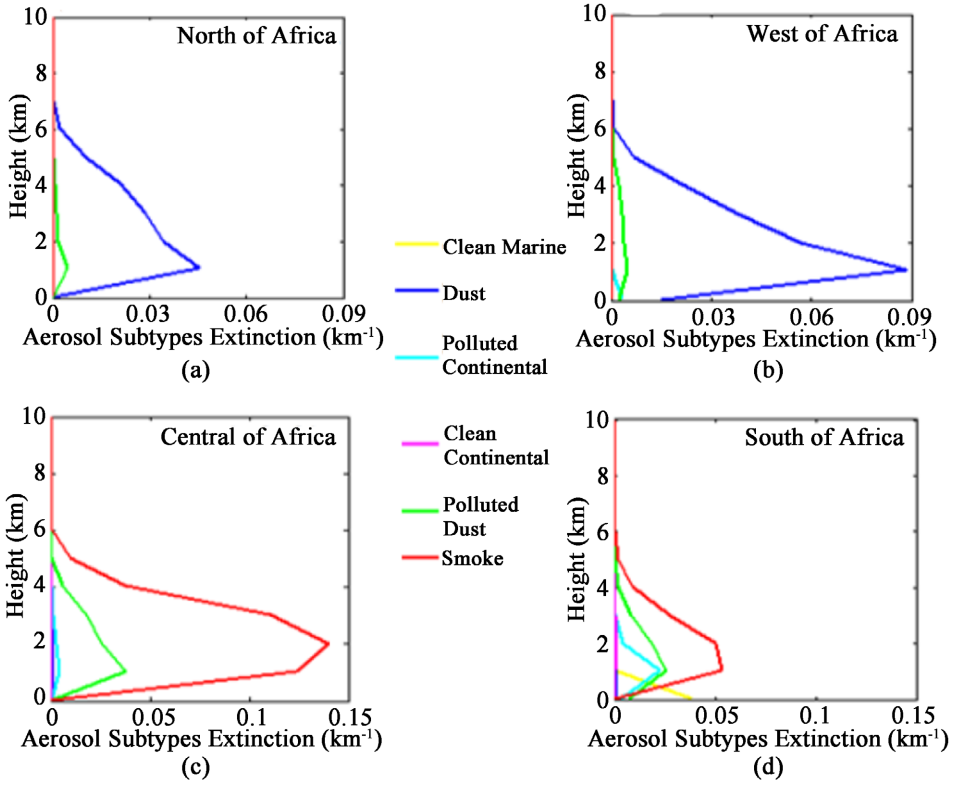

Figure 2. Aerosol subtype extinction average in 40 regions in North of Africa (a), West of Africa (b), Central Africa (c), and South of Africa (d) from 2008 to 2011.

The dust and biomass burning aerosol particles have different effects on cloud formation [27]. The dust aerosols are remarkably changed cloud properties, whereby the previous studies indicated the reduction of the cloud optical depth, liquid water path, and the effective particle size in altocumulus and Cirrus clouds [37]. The cloud subtype extinction with considerable high values is Altocumulus (Ac) in North (0.0139 km^{-1}) (**Figure 2(a)**), Central (0.058 km^{-1}) (**Figure 3(b)**) and Western (0.013 km^{-1}) (**Figure 3(c)**) of Africa between 3.5 km to 5 km, which reveals a significant role that aerosols may have in middle clouds in those regions. In contrast with North, Central, West of Africa, the cloud subtype extinction with high values is low overcast transparent (0.76 km^{-1}) below 1 km in South of Africa (**Figure 3(d)**), due to the coastal regions considered in this study. There are considerable low extinctions of other cloud subtypes (low overcast opaque, transition stratocumulus, low broken cumulus, altostratus opaque, and deep convective opaque) in all four regions (NA, WA, CA and SA).

The high dust amount is mostly concentrated at heights close to the surface in Sahara desert [38], which is in agreement with our results as shown by optical properties. The aerosol extinction, backscatter and depolarization ratio coefficients increase from the surface to 1.2 km and decrease from 1.2 km to the upper layers in both WNA and CSA at both 532 nm and 1064 nm (**Figure 4(a)**, **Figure 4(b)**, **Figure 4(c)**). The maximum aerosol extinction coefficients of 0.07 km^{-1} and 0.08 km^{-1} (**Figure 4(a)**), while the maximum aerosol backscatter coefficients

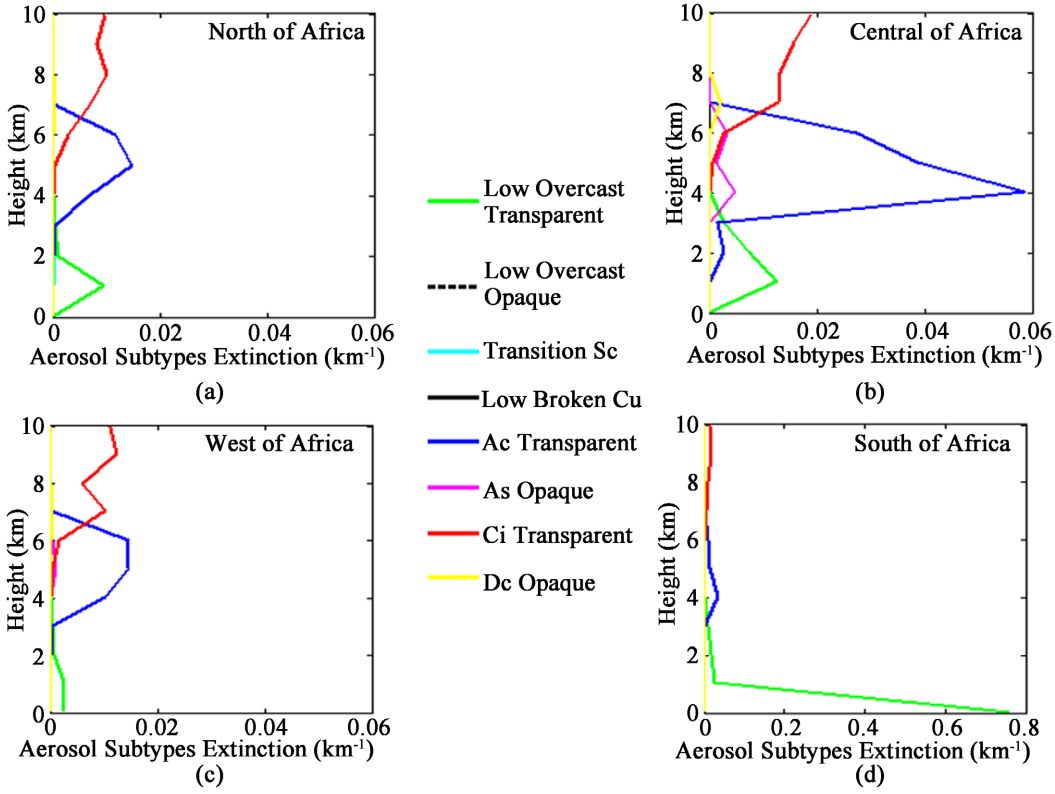

Figure 3. Cloud subtype extinction average in North of Africa (a), West of Africa (b), Central Africa (c), and South of Africa (d) from 2008 to 2011.

of 0.0017 $km^{-1}\cdot sr^{-1}$ and 0.0015 $km^{-1}\cdot sr^{-1}$ (**Figure 4(b)**) are found around 1 km with 532 nm and 1064 nm respectively in WNA. The maximum aerosol extinction coefficients of 0.13 km^{-1} and 0.14 km^{-1} (**Figure 4(a)**), while the maximum aerosol backscatter coefficients of 0.0021 $km^{-1}\cdot sr^{-1}$ and 0.0033 $km^{-1}\cdot sr^{-1}$ (**Figure 4(b)**) are found around 1 km with 532 nm and 1064 nm respectively in CSA. This shows that there is a remarkable sensitivity of 532 nm and 1064 nm wavelengths on the extinction and backscatter coefficients. The aerosol extinctions at 532 nm are greater than at 1064 nm at all altitudes due to the fact that the aerosols are primarily products of fresh biomass burning and industrial pollution, which contain relatively small particles in Southern Africa [39]. The dominated smoke aerosol regions have high extinction and backscatter than dominated dust aerosol regions. We have realized also that the dust extinction and backscatter coefficients are higher than those of smoke at the height of 4 km to 6 km. This is mainly due to the aerosol and cloud interactions in the middle cloud level. This reveals also different impacts of dust and smoke aerosols on clouds. The dust and smoke optical properties from the surface to upper layers change with height. The aerosol physical and chemical properties are height dependent [26]. The aerosol depolarization ratio in dominated dust aerosol region (maximum of 0.25 in WNA) is significantly higher than in dominated smoke region (maximum of 0.05 in CSA) (**Figure 4(c)**). This shows that the aerosol depolarization ratio can be used to identify aerosol types, as indicated in the previous study by

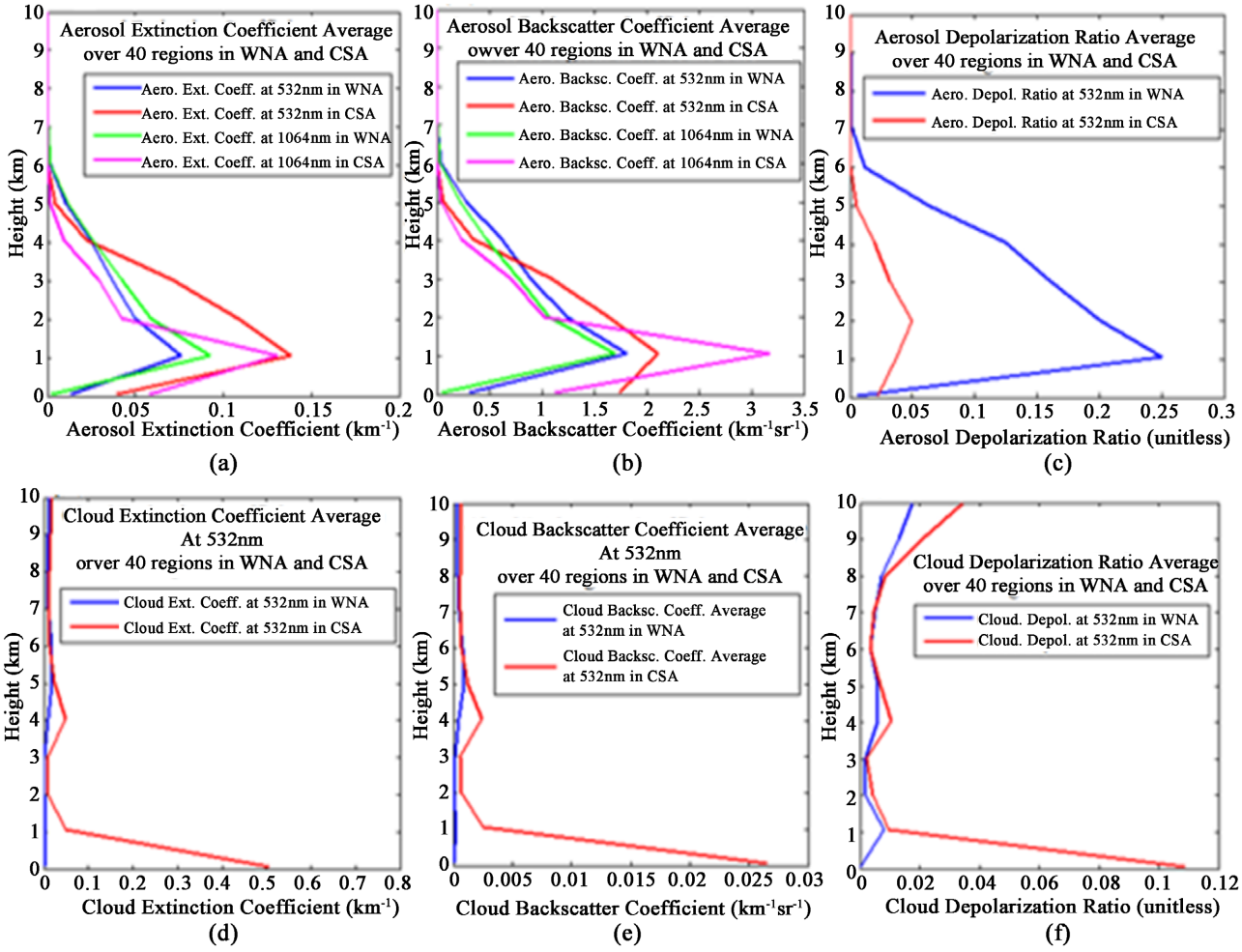

Figure 4. The average of aerosol (a)-(c) and cloud (d)-(f) optical properties in 20 regions in WNA and 20 regions in CSA from 2008 to 2011.

Omar *et al.* [12]. The high and low of aerosol depolarization contribute to the decrease and increase of both scattering and absorption of dust and smoke aerosols, respectively. The significant low aerosol depolarization from 7 km indicates the presence of the mixture of dust and smoke aerosols. The low depolarization may reveal also the decrease of the size of the dust aerosols as very small particles do not significantly depolarize laser light [14]. This shows that dust particles are considerable larger than smoke particles below 7 km. The cloud optical properties in dominated smoke region (CSA) are considerably higher than in dominated dust aerosol region (WNA) whereby high values are found below 1 km (**Figure 4(d)**, **Figure 4(e)**), **Figure 4(f)**). The cloud extinction (**Figure 4(d)**) and cloud backscatter (**Figure 4(e)**) coefficients indicate smooth changes with height, while there is a remarkable increase of cloud depolarization ratio with height in high clouds (**Figure 4(f)**) mainly due to the presence of Cirrus (Ci) ice cloud.

In a previous study, we found that cloud types and cloud fraction change by region in Africa [35]. This is the reason we have also considered the variability of

vertical aerosol and cloud optical properties in low, middle and high clouds (Figure 5) by a region in North of Africa (NA), West of Africa (WA), Central of Africa (CA) and South of Africa (SA) at 532 nm. The high and low values of both aerosol extinction coefficients are found in CA (0.11 km^{-1}, 0.05 km^{-1}) and NA (0.028 km^{-1}; 0.029 km^{-1}) in low and middle clouds (Figure 5(a)) respectively. The high and low values of aerosol backscatter coefficients are found in CA (0.0016 $km^{-1}\cdot sr^{-1}$) and NA (0.0007 $km^{-1}\cdot sr^{-1}$) respectively in low clouds, while they are found in CA (0.0017 $km^{-1}\cdot sr^{-1}$) and SA (0.0003 $km^{-1}\cdot sr^{-1}$) in middle clouds (Figure 5(b)). There are significant differences of aerosol depolarization ratio in dust and biomass burning regions, whereby high and low values are found in WA (0.16 and 0.17) and CA (0.03 and 0.01) in both low and middle clouds respectively (Figure 5(c)). This shows that aerosol depolarization may be used as an indicator of aerosol subtypes. This is in agreement with the previous study by Tesche *et al.* [40], whereby they demonstrated that the particle depolarization ratio at 532 nm maybe used to separate aerosol types. The cloud extinction, cloud backscatter, and cloud depolarization ratio coefficients are significantly high in SA compared to CA, WA, and NA in low cloud, while no significant differences in middle and high clouds for all regions (Figure 5(d), Figure 5(e), Figure 5(f)). This is due probably to the large fraction of low overcast transparent cloud in SA as indicated by Figure 3(d). It is clear that the cloud depolarization ratios for SA, CA, WA, and NA increase in high clouds, whereby high and low values are found in CA due to a high fraction of Cirrus clouds as

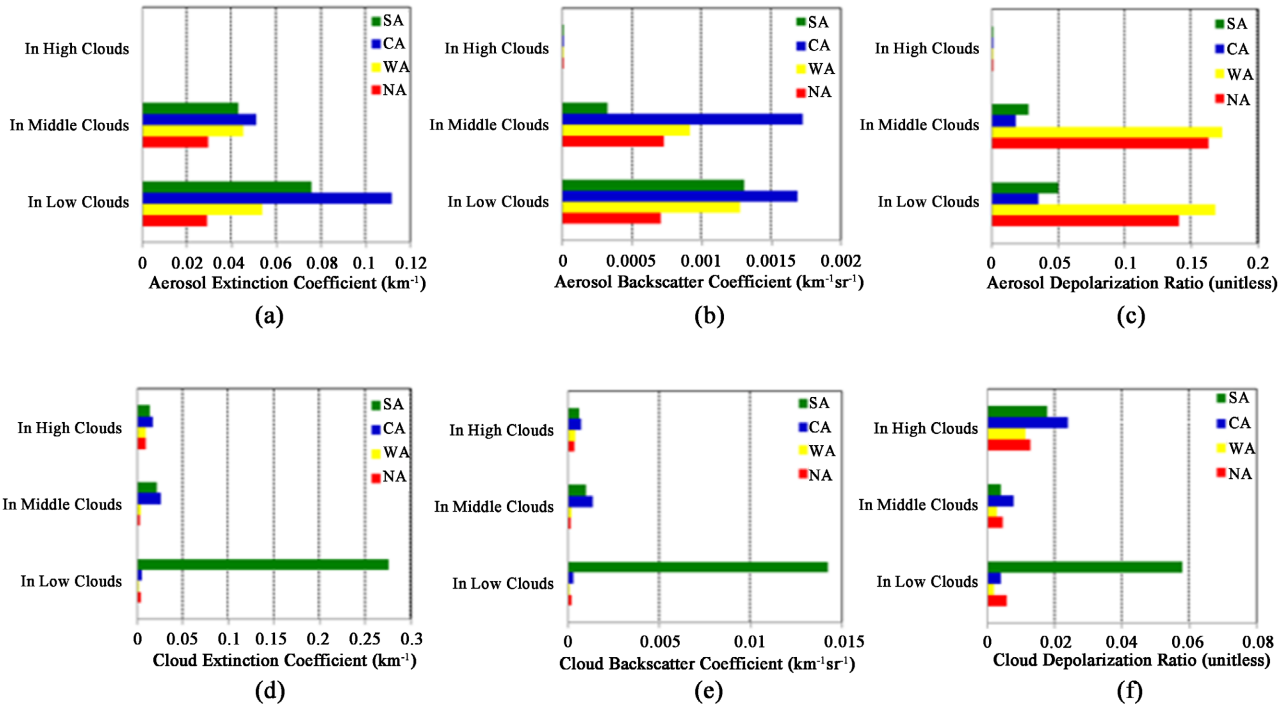

Figure 5. The average of aerosol optical properties (a)-(c) and cloud optical properties (d)-(f) at 532 nm in low, middle, and high cloud levels in 40 regions of South of Africa (SA), Central of Africa (CA), West of Africa (WA) and North of Africa (NA) from 2008 to 2011.

demonstrated by Figure 3(b). The high and low values of cloud depolarization ratio found in CSA and WNA are related to the high and low fraction of high clouds in CSA and WNA (Figure 5(f)), respectively.

The increase of cloud depolarization maybe used as an indicator of ice clouds. The low and high cloud depolarization ratio maybe used as an indicator of liquid cloud and ice clouds, respectively, in NA, WA, and CA. In contrast to the other three regions, the cloud depolarization in SA maybe used as an indicator of low and ice clouds in middle and high cloud levels and not in low cloud levels.

4. Summary and Conclusions

Several studies have been done on dust vertical distribution in West and North of Africa due mainly to the presence of Sahara desert and Sahel region, but few studies have investigated the vertical distribution of smoke aerosols in Central and South of Africa. In this study, we tried to fill that gap by comparing the vertical distribution of dust and smoke aerosols in West-North of Africa (WNA) and Central-South of Africa (CSA) as the climatology aspect. In contrast to many previous studies whereby they evaluated large scale, we have focused on many regions as possible to understand deep aerosol vertical distribution at a local scale.

The main objective of this study is to compare the vertical profile of aerosol and cloud optical properties and to investigate the relationship between the vertical structure of aerosol and cloud optical properties in dominated dust and smoke aerosol regions. The climatology of dust and smoke aerosols optical properties in West-North (20 regions) and Central-South of Africa (20 regions) was studied using LIVAS data. We have used the data of six aerosol and cloud optical properties based on lidar climatology of Vertical Aerosol Structure for space-based lidar simulation studies (LIVAS). We have selected twenty regions located in dominated dust aerosols in North and West of Africa (WNA) and twenty other regions with high concentration of smoke aerosols in Central and South of Africa (CSA).

The annual average of aerosol types shows that the dust and smoke aerosols are dominating in WNA and CSA, respectively. The new major findings show considerable high sensitivity of dust and smoke aerosols at 532 nm and 1064 nm and accompanied by the changes of optical properties with height. The aerosol extinction, backscatter, and depolarization ratio coefficient values of both dust and smoke increase from the surface to 1.2 km and then decrease from 1.2 km to 6 km. The smoke extinction and backscatter coefficient values are higher than those of dust aerosols from the surface to 4 km, whereas the dust extinction and backscatter coefficient values are high than those of smoke aerosols from 4 km to 6 km. This shows that the variability of the meteorological effects on dust and smoke aerosols are different due mainly to their optical, physical, and chemical properties. The aerosol depolarization property shows an exception whereby dust aerosols have high depolarization ratio than smoke aerosols from the sur-

face to the upper layers. The cloud optical properties in dominated smoke region (CSA) are considerably higher than in dominated dust aerosol region (WNA). There is a smooth change in the height of cloud extinction and cloud backscatter coefficient in both WNA and CSA, while there is a significant difference in cloud depolarization in the two regions. The cloud depolarization in smoke-dominated regions is considerably high than that in dust-dominated regions, especially between the surface and 1 km altitude. In the middle clouds, there is almost no difference in cloud optical properties in WNA and CSA, while in high cloud levels there is a remarkable increase in cloud depolarization in both WNA and CSA mainly due to the increase of ice cloud particles. This reveals that cloud depolarization may be used as an indicator of ice clouds. The cloud depolarization in CSA is always higher than that in WNA from low to high cloud levels. The altocumulus is the cloud with high extinction in NA, WA, and CA, while it is low overcast transparent in SA.

Acknowledgements

The first author would like to thank Dr. Vassilis Amiridis for his kind assistance on how to have access to LIVAS data used in this study and we thank all their team for their sharing scientific spirit. We are also thankful to the anonymous reviewers for their useful, insightful, and constructive criticisms, which have significantly improved this paper.

Conflicts of Interest

The authors declare no conflicts of interest regarding the publication of this paper.

References

[1] Ntwali, D. and Chen, H. (2018) Diurnal Spatial Distributions of Aerosol Optical and Cloud Micro-Macrophysics Properties in Africa Based on MODIS Observations. *Atmospheric Environment*, **182**, 252-262. https://doi.org/10.1016/j.atmosenv.2018.03.054

[2] Schütz, L., Jaenicke, R. and Pietrek, H. (1981) Saharan Dust Transport over the North Atlantic Ocean. In: Péwé, T.L., Ed., *Desert Dust*, Geological Society of America, Boulder, Special Paper, Vol. 186, 87-100. https://doi.org/10.1130/SPE186-p87

[3] Swap, R., Ulanski, S., Cobbett, M. and Garstang, M. (1996) Temporal and Spatial Characteristics of Saharan Dust Outbreaks. *Journal of Geophysical Research*, **101**, 4205-4220. https://doi.org/10.1029/95JD03236

[4] Mattis, I., Ansmann, A., Muller, D., Wandinger, U. and Althausen, D. (2002) Dual-Wavelength Raman Lidar Observations of the Extinction-to-Backscatter Ratio of Saharan Dust. *Geophysical Research Letters*, **29**, 20-1-20-4. https://doi.org/10.1029/2002GL014721

[5] Prospero, J.M., Ginoux, P., Torres, O., Nicholson. S.E. and Gill, T.E. (2002) Environmental Characterization of Global Sources of Atmospheric Soil Dust Identified with the NIMBUS 7 Total Ozone Mapping Spectrometer (TOMS) Absorbing Aerosol Product. *Review Geophysics*, **40**, 2-1-2-31.

https://doi.org/10.1029/2000RG000095

[6] Engelstaedter, S. and Washington, R. (2007) Temporal Controls on Global Dust Emissions: The Role of Surface Gustiness. *Geophysical Research Letters*, **34**, L15805. https://doi.org/10.1029/2007GL029971

[7] Liu, Z., Omar, A., Vaughan, M., Hair, J., Kittaka, C., Hu, Y., Powell, K., Trepte, C., Winker, D., Hostetler, C., Ferrare, R. and Pierce, R. (2008) CALIPSO Lidar Observations of the Optical Properties of Saharan Dust: A Case Study of Long-Range Transport. *Journal of Geophysical Research*, **113**, D07207. https://doi.org/10.1029/2007JD008878

[8] Dubovik, O., Holben, B., Eck, T.F., Smirnov, A., Kaufman, Y.J., King, M.D., Tanré, D. and Slutsker, I. (2002) Variability of Absorption and Optical Properties of Key Aerosol Types Observed in Worldwide Locations. *Journal of the Atmospheric Sciences*, **59**, 590-608. https://doi.org/10.1175/1520-0469(2002)059<0590:VOAAOP>2.0.CO;2

[9] Eck, T.F., Holben, B.N., Ward, D.E., Dubovik, O., Reid, J.S., Smirnov, A., Mukelabai, M.M., Hsu, N.C., O'Neill, N.T. and Slutsker, I. (2001) Characterization of the Optical Properties of Biomass Burning Aerosols in Zambia during the 1997 ZIBBEE Field Campaign. *Journal of Geophysical Research*, **106**, 3425-3448. https://doi.org/10.1029/2000JD900555

[10] Levine, J.S. (1991) Global Biomass Burning: Atmospheric, Climatic, and Biospheric Implications. MIT Press, Cambridge. https://doi.org/10.7551/mitpress/3286.001.0001

[11] Hodnebrog, Ø., Myhre, G., Sillmann, J. and Samset, B.H. (2016) Local Biomass Burning Is a Dominant Cause of the Observed Precipitation Reduction in Southern Africa. *Nature Communications*, **7**, Article No. 11236. https://doi.org/10.1038/ncomms11236

[12] Omar, A., Winker, D., Vaughan, M., Hu, Y., Trepte, C., Ferrare, R., Lee, K., Hostetler, C., Kittaka, C., Rogers, R., Kuehn, R. and Liu, Z. (2009) The CALIPSO Automated Aerosol Classification and Lidar Ratio Selection Algorithm. *Journal of Atmospheric and Oceanic Technology*, **26**, 1994-2014. https://doi.org/10.1175/2009JTECHA1231.1

[13] Amiridis, V., Marinou, E., Tsekeri, A., Wandinger, U., Schwarz, A., Giannakaki, E., Mamouri, R., Kokkalis, P., Binietoglou, I., Solomos, S., Herekakis, T., Kazadzis, S., Gerasopoulos, E., Balis, D., Papayannis, A., Kontoes, C., Kourtidis, K., Papagiannopoulos, N., Mona, L., Pappalardo, G., Le Rille, O. and Ansmann, A. (2015) LIVAS: A 3-D Multi-Wavelength Aerosol/Cloud Climatology Based on CALIPSO and EARLINET. *Atmospheric Chemistry and Physics Discussions*, **15**, 2247-2304. https://doi.org/10.5194/acpd-15-2247-2015

[14] Ansmann, A., Bösenberg, J., Chaikovsky, A., Comerón, A., Eckhardt, S., Eixmann, R., Freudenthaler, V., Ginoux, P., Komguem, L., Linné, H., Lopez Marquez, M.A., Matthias, V., Mattis, I., Mitev, V., Müller, D., Music, S., Nickovic, S., Pelon, J., Sauvage, L., Sobolewsky, P., Srivastava, M.K., Stohl, A., Torres, O., Vaughan, G., Wandinger, U. and Wiegner, M. (2003) Long-Range Transport of Saharan Dust to Northern Europe: The 11-16 October 2001 Outbreak Observed with EARLINET. *Journal of Geophysical Research*, **108**, 4873. https://doi.org/10.1029/2003JD003757

[15] Müller, D., Mattis, I., Wandinger, U., Ansmann, A., Althausen, D., Dubovik, O., Eckhardt, S. and Stohl, A. (2003) Saharan Dust over a Central European EARLINET-AERONET Site: Combined Observations with Raman Lidar and Sun Photometer. *Journal of Geophysical Research*, **108**, 4345. https://doi.org/10.1029/2002JD002918

[16] Balis, D.S., Amiridis, V., Nickovic, S., Papayannis, A. and Zerefos, C. (2004) Optical

Properties of Saharan Dust Layers as Detected by a Raman Lidar at Thessaloniki, Greece. *Geophysical Research Letters*, **31**, L13104. https://doi.org/10.1029/2004GL019881

[17] Kovalev, V.A. and Eichinger, W.E. (2004) Elastic Lidar. Theory, Practice and Analysis Methods. Wiley-Interscience, Hoboken, 615 p. https://doi.org/10.1002/0471643173

[18] Papayannis, A., Balis, D., Amiridis, V., Chourdakis, G., Tsaknakis, G., Zerefos, C., Castanho, A.D.A, Nickovic, S., Kazadzis, S. and Grabowski, J. (2005) Measurements of Saharan Dust Aerosols over the Eastern Mediterranean Using Elastic Backscatter-Raman Lidar, Spectrophotometric and Satellite Observations in the Frame of the EARLINET Project. *Atmospheric Chemistry and Physics*, **5**, 2065-2079. https://doi.org/10.5194/acp-5-2065-2005

[19] Goudie, A.S. and Middleton, N.J. (2001) Saharan Dust Storms: Nature and Consequences. *Earth Sciences Review*, **56**, 179-204. https://doi.org/10.1016/S0012-8252(01)00067-8

[20] Kallos, G., Papadopoulos, A., Katsafados, P. and Nickovic, S. (2006) Transatlantic Saharan Dust Transport: Model Simulation and Results. *Journal of Geophysical Research*, **111**, D09204. https://doi.org/10.1029/2005JD006207

[21] Keil, A. and Haywood, J.M. (2003) Solar Radiative Forcing by Biomass Burning Aerosol Particles during SAFARI 2000: A Case Study Based on Measured Aerosol and Cloud Properties. *Journal of Geophysical Research*, **108**, 8467. https://doi.org/10.1029/2002JD002315

[22] Bauer, S., Bierwirth, E., Esselborn, M., Petzold, A., Macke, A., Trautmann, T. and Wendisch, M. (2011) Airborne Spectral Radiation Measurements to Derive Solar Radiative Forcing of Saharan Dust Mixed with Biomass Burning Smoke Particles. *Tellus B*, **63**, 742-750. https://doi.org/10.1111/j.1600-0889.2011.00567.x

[23] Barbosa, P., Stroppiana, D., Grégoire, J.M. and Cardoso Pereira, J. (1999) An Assessment of Vegetation Fire in Africa (1981-1991): Burned Areas, Burned Biomass, and Atmospheric Emissions. *Global Biogeochemical Cycles*, **13**, 933-950. https://doi.org/10.1029/1999GB900042

[24] Tesche, M., Groß, S., Ansmann, A., Müller, D., Althausen, D., Freudenthaler, V., Weinzierl, B., Veira, A. and Petzold, A. (2011) Optical and Microphysical Properties of Smoke over Cape Verde Inferred from Multiwavelength Lidar Measurements. *Tellus B*, **63**, 649-676. https://doi.org/10.1111/j.1600-0889.2011.00548.x

[25] Kalashnikova, O.V. and Sokolik, I.N. (2002) Importance of Shapes and Composition of Wind-Blown Dust Particles for Remote Sensing at Solar Wavelengths. *Geophysical Research Letters*, **29**, 38-1-38-4. https://doi.org/10.1029/2002GL014947

[26] Ackerman, J. (1998) The Extinction-to-Backscatter Ratio of Tropospheric Aerosol: A Numerical Study. *Journal of Atmospheric and Oceanic Technology*, **15**, 1043-1050. https://doi.org/10.1175/1520-0426(1998)015<1043:TETBRO>2.0.CO;2

[27] Ansmann, A., Baars, H., Tesche, M., Müller, D., Althausen, D., Engelmann, R., Pauliquevis, T. and Artaxo, P. (2009) Dust and Smoke Transport from Africa to South America: Lidar Profiling over Cape Verde and the Amazon Rainforest. *Geophysical Research Letters*, **36**, L11802. https://doi.org/10.1029/2009GL037923

[28] Kaufman, Y.J., Koren, I., Remer, L.A., Tanré, D., Ginoux, P. and Fan, S. (2005) Dust Transport and Deposition Observed from the Terra-Moderate Resolution Imaging Spectroradiometer (MODIS) Spacecraft over the Atlantic Ocean. *Journal of Geophysical Research*, **110**, D10S12. https://doi.org/10.1029/2003JD004436

[29] Tsikerdekis, A., Zanis, P., Steiner, A.L., Solmon, F., Amiridis, V., Marinou, E.,

Katragkou, E., Karacostas, T. and Foret, G. (2016) Dust Size Parameterization in RegCM4: Impact on Aerosol Burden and Radiative Forcing. *Atmospheric Chemistry and Physics Discussions*, 35 p. https://doi.org/10.5194/acp-2016-434

[30] Vaughan, M.A, Powell, K.A., Kuehn, R.E., Young, S.A., Winker, D.M., Hostetler, C.A., Hunt, W.H., Liu, Z., Mcgill, M.J. and Getzewich, B.J. (2009) Fully Automated Detection of Cloud and Aerosol Layers in the CALIPSO Lidar Measurements. *Journal of Atmospheric and Oceanic Technology*, **26**, 2034-2050. https://doi.org/10.1175/2009JTECHA1228.1

[31] Liu, X.H., Penner, J.E. and Wang, M.H. (2009) Influence of Anthropogenic Sulfate and Black Carbon on Upper Tropospheric Clouds in the NCAR CAM3 Model Coupled to the IMPACT Global Aerosol Model. *Journal of Geophysical Research*, **114**, D03204. https://doi.org/10.1029/2008JD010492

[32] Woodward, S. (2001) Modeling the Atmospheric Life-Cycle and Radiative Impact of Mineral Dust in the Hadley Centre Climate Model. *Journal of Geophysical Research*, **106**, 18155-18166. https://doi.org/10.1029/2000JD900795

[33] Prospero, J.M. and Lamb, P.J. (2003) African Droughts and Dust Transport to the Caribbean: Climate Change Implications. *Science*, **302**, 1024-1027. https://doi.org/10.1126/science.1089915

[34] Ntwali, D., Mugisha, E., Vuguziga, F. and Kakpa, D. (2016) Liquid and Ice Water Content in Clouds and Their Variability with Temperature in Africa Based on ERA-Interim, JRA-55, MERRA and ISCCP. *Meteorology and Atmospheric Physics*, **129**, 17-34. https://doi.org/10.1007/s00703-016-0447-z

[35] Freudenthaler, V., Esselborn, M., Wiegner, M., Heese, B., Tesche, M., Ansmann, A., D. Müller, D., Althausen, D., Wirth, M., Fix, A., Ehret, G., Knippertz, P., Toledano, C., Gasteiger, J., Garhammer, M. and Seefeldner, M. (2009) Depolarization Ratio Profiling at Several Wavelengths in Pure Saharan Dust during SAMUM 2006. *Tellus B*, **61**, 165-179. https://doi.org/10.3402/tellusb.v61i1.16821

[36] Liu, Y., Huang, J., Shi, G., Takamura, T., Khatri, P., Bi, J., Shi, J., Wang, T., Wang, X. and Zhang, B. (2011) Aerosol Optical Properties and Radiative Effect Determined from Sky-Radiometer over Loess Plateau of Northwest China. *Atmospheric Chemistry and Physics*, **11**, 11455-11463. https://doi.org/10.5194/acp-11-11455-2011

[37] Wang, W., Sheng, L., Jin, H. and Han, Y. (2015) Dust Aerosols Effects on Cirrus and Altocumulus Clouds in Northwest China. *Journal of Meteorological Research*, **29**, 793-805. https://doi.org/10.1007/s13351-015-4116-9

[38] Marinou, E., Amiridis, V., Binietoglou, I., Tsikerdekis, A., Solomos, S., Proestakis, E., Konsta, D., Papagiannopoulos, N., Tsekeri, A., Vlastou, G., Zanis, P., Balis, D., Wandinger, U. and Ansmann, A. (2017) Three-Dimensional Evolution of Saharan Dust Transport towards Europe Based on a 9-Year EARLINET-Optimized CALIPSO Dataset. *Atmospheric Chemistry and Physics*, **17**, 5893-5919. https://doi.org/10.5194/acp-17-5893-2017

[39] McGill, M.J., Hlavka, D.L., Hart, W.D., Welton, E.J. and Campbell, J.R. (2003) Airborne Lidar Measurements of Aerosol Optical Properties during SAFARI-2000. *Journal of Geophysical Research Atmospheres*, **108**, 8493. https://doi.org/10.1029/2002JD002370

[40] Tesche, M., Ansmann, A., Müller, D., Althausen, D., Engelmann, R., Freudenthaler, V. and Groß, S. (2009) Vertically Resolved Separation of Dust and Smoke over Cape Verde Using Multiwavelength Raman and Polarization Lidars during Saharan Mineral Dust Experiment 2008. *Journal of Geophysical Research*, **114**, D13202. https://doi.org/10.1029/2009JD011862